Proc. Natl. Acad. Sci. USA
Vol. 84, pp. 3936–3940, June 1987
Neurobiology

The retinal ganglion cell mosaic defines orientation columns in striate cortex

(visual cortex/neural modeling)

ROBERT E. SOODAK

The Rockefeller University, 1230 York Avenue, New York, NY 10021

Communicated by Floyd Ratliff, March 9, 1987 (received for review November 11, 1986)

ABSTRACT **A computer simulation was used to demonstrate that the tangential organization of orientation columns is a natural consequence of the orderly projection of the mosaic of retinal ganglion cells onto the visual cortex. Parameters of the simulation were taken from published anatomical and electrophysiological data, and the resulting columnar organization of the simulated visual cortex shows many similarities with observations from animals. The model is able to account for a variety of experimental observations, including the presence of orientation columns in visually inexperienced animals.**

One of the striking features of the cortical representation of the visual field is the grouping of neurons with similar preferred orientations into the orientation columns described by Hubel and Wiesel (1, 2). This columnar organization is already present in kittens at the time of eye opening and must, therefore, be determined by intrinsic developmental processes that are independent of visual experience (3–6). In a previous report, I showed how the orientation tuning of visual cortex neurons could be calculated from the pattern of convergence of on- and off-center afferents (7). Using this calculation procedure, I show here that the tangential organization of the orientation columns is a natural consequence of the orderly projection of the retinal ganglion cell mosaic onto the cortex.

Wässle and his collaborators (8, 9) have shown that retinal ganglion cells (RGCs) of the cat are arranged in a lattice-like mosaic with regular cell-to-cell spacings. Similar arrangements were found for both the β (8) and α (9) morphological types, which Boycott and Wässle (10) and Wässle *et al.* (11) have shown to correspond to the X and Y physiological types (12–15), respectively. For both the X and Y cells, on- and off-center RGCs form their own lattices, and the on and off lattices are superimposed independently of each other (8, 9). Since the signals from RGCs are relayed through the lateral geniculate nucleus (LGN) without substantial modification (16–19), the RGC mosaic represents the pattern of visual input to the cortex. Thus, as emphasized by Wässle *et al.* (8), the RGC mosaic serves as an important constraint on the construction of cortical receptive fields.

THE SIMULATION

What I present here is the result, by computer simulation, of the developmental process whereby the RGC mosaic projects retinotopically by way of the LGN onto the cortex. The simulation begins with two sets of coordinates, corresponding to the retinal positions of the on- and off-center RGCs. The receptive fields of the cortical neurons are then defined as a convergence of RGC inputs, and their responses are calculated using the procedure described in a previous report (7). The positions of the RGCs in the retinal mosaic were measured from figure 9 of Wässle *et al.* (8) after photographic enlargement and were corrected for tissue shrinkage by the areal shrinkage factor of 0.5 provided by the authors. Other parameters of the simulation were also obtained from experimental data. A cortical magnification factor of 0.1 (mm^2 of cortex per $degree^2$ of visual field) was obtained from figure 12 of Tusa *et al.* (20), for the eccentricity of 33°, where the retinal sample of Wässle *et al.* (8) was taken. To simulate the mapping of the RGC mosaic onto the cortex, it is necessary to specify the strength of connection between a given RGC and target cortical neuron, which varies as a function of the distance between their retinotopic positions. I refer to this as the "distance function." Since the X mosaic was used for the simulation, the distance function represents the spread of X-geniculate afferents tangential to the cortical surface. Ferster and LeVay (21) give a value of approximately 0.5 mm for the lateral spread of X-cell afferents in striate cortex. Humphrey *et al.* (22) report that axon arbors of X cells cover a surface area of 0.6–0.9 mm^2, which, assuming a circular distribution, corresponds to diameters of 0.87–1.07 mm. For the simulation, a Gaussian distance function was used; the function fell to 25% of its peak value at a diameter of 0.5 mm and to 1% of its peak value at a diameter of 0.9 mm, at which point it was truncated. Using this distance function, each simulated cortical neuron receives input from an average of 27 afferents. The density and positions of the simulated cortical neurons are important only in that they represent sampling points of a continuous function defined by the afferent input pattern. I used a sampling density of 30 by 50 cortical neurons within a region of 0.6 × 1 mm. Edge effects were avoided by restricting the cortical neurons to lie within a boundary 0.45 mm inside the region over which the RGC mosaic was defined.

Other factors, omitted from the simulation for the sake of simplicity, may also influence the blueprint for the orientation columns. Perhaps the most important of these is the Y-cell mosaic. Both X and Y cells provide input to striate cortex (21–26), and there are no compelling reasons to believe that the Y-cell input is not important in determining the response properties of kitten cortical neurons. Another simplification is that in calculating the responses of the simulated cortical neurons, I assumed radial symmetry of the RGC receptive fields. Experimental data indicate that RGC receptive fields are, in fact, slightly elongated ellipses (27–30) and have average major-to-minor axis ratios of 1.2–1.3. Based on similar overrepresentations of radial-preferred orientations in the retina and cortex, Leventhal (31, 32) and Schall *et al.* (33) have suggested that this slight elongation of RGC receptive fields is responsible for determining the orientation preferences of neurons in the visual cortex. However, as pointed out by Leventhal (32), the elongation of

The publication costs of this article were defrayed in part by page charge payment. This article must therefore be hereby marked "*advertisement*" in accordance with 18 U.S.C. §1734 solely to indicate this fact.

Abbreviations: RGC, retinal ganglion cell; LGN, lateral geniculate nucleus.

RGC receptive fields cannot account for the defining property of orientation columns—i.e., the grouping of cortical neurons with similar orientation preferences—as there is no such grouping in the retina. Although the slight elongation of RGC receptive fields might confer a general tendency toward radial preferred orientations in the cortex, other influences, such as anisotropy of the cortical magnification factor (34, 35), might also contribute to this tendency by distorting the mapping of the RGC mosaic onto the cortex.

The distribution of preferred orientations on the simulated cortical surface was determined as follows. A connectivity map between the RGCs and cortical neurons was determined using the distance function described above. The strength of the connection between a given RGC and a target cortical neuron depended only on the distance between their retinotopic positions and was independent of all other connections. This defined a receptive field for each cortical cell that was a linear combination of on- and off-center RGC receptive fields. On-center RGCs were assumed to respond at a 0° phase delay and off-center RGCs at a 180° phase delay. The responses of each cortical neuron were calculated at 12 equally spaced orientations at a spatial frequency of 0.1 cycles per degree. The result is shown in Fig. 1, which depicts preferred orientations on a tangential view of the simulated cortex. The three types of shading symbols (-, /, \) indicate the positions of cortical neurons responding best within three 60° ranges of orientation. It is apparent from this figure that preferred orientations are represented in an orderly, columnar fashion, and there is a strong tendency of nearby neurons to respond best at similar orientations. Fig. 2 shows the preferred orientations, calculated here with 1° resolution, of neurons in the three vertical rows indicated by arrows at the top of Fig. 1. This representation can be thought of as a simulation of preferred orientations along electrode penetrations tangential to the cortical surface. The tendency of nearby neurons to have similar preferred orientations is again apparent. Also evident is a generally smooth and monotonic change of preferred orientation with position, except for occasional jumps or a reversal of the direction of change. These features are similar to experimental observations in striate cortex (2, 36–39).

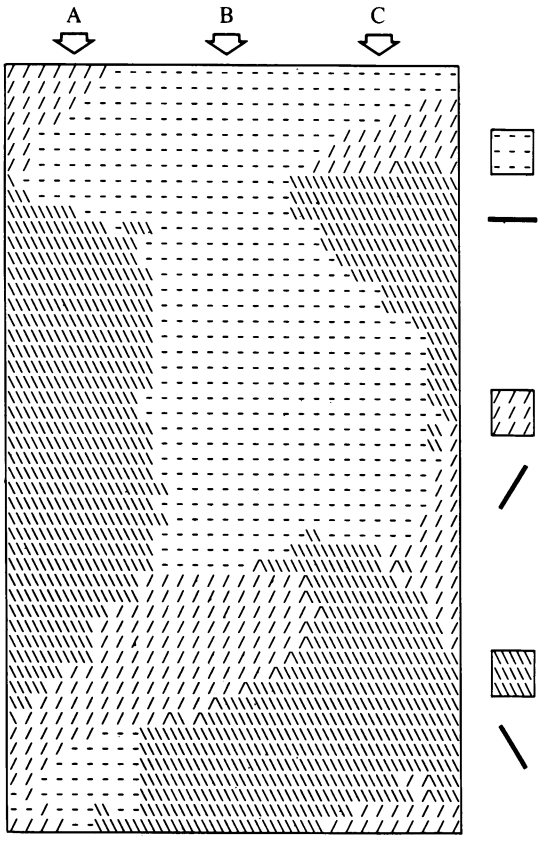

FIG. 1. Distribution of preferred orientations on a simulated cortical surface (0.6 × 1 mm). The three types of shading symbols (-, /, \) indicate the positions of cortical neurons responding best within three 60° ranges of orientation.

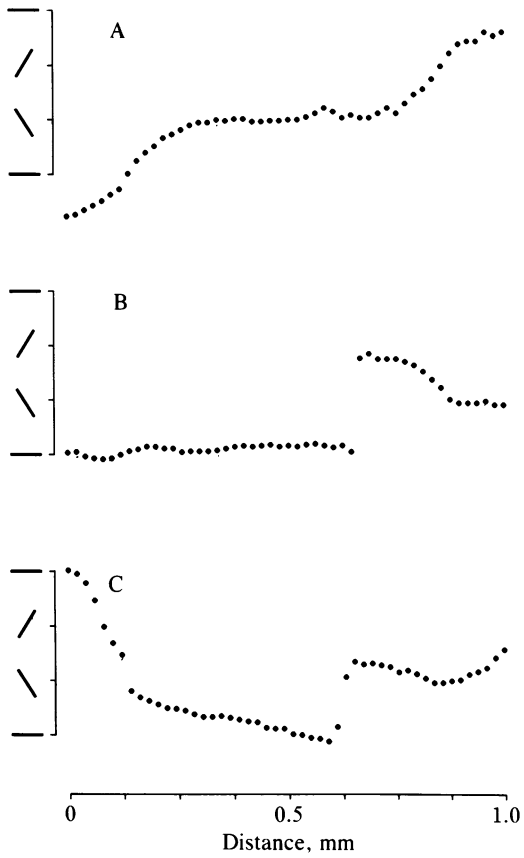

FIG. 2. Preferred orientations of neurons in the vertical rows indicated by arrows A–C at the top of Fig. 1, calculated with 1° resolution. This representation can be thought of as a simulation of preferred orientations along electrode penetrations tangential to the cortical surface.

The response properties of individual neurons in the simulated striate cortex are illustrated in Fig. 3. A measure of the sharpness of the orientation tuning, $(R_{max} - R_{min})/(R_{max} + R_{min})$, where R_{max} and R_{min} are, respectively, the maximum and minimum responses as a function of orientation, is shown in Fig. 3*A* for the vertical row of neurons labeled B in Fig. 1. This measure varies from zero, for a neuron with no orientation preference, to a maximum of one. The sharpness of tuning is shown for spatial frequencies of 0.1 and 0.25 cycles per degree. There are two important features of these results. First, it is apparent that neurons with the highest sensitivity to the orientation of the stimulus are grouped together in clusters. The occurrence in clusters of orientation-sensitive cells has, in fact, been reported for visually inexperienced cats (40). The second important feature is the spatial frequency dependence of the sharpness of tuning. As cortical neurons of kittens are more broadly tuned to spatial frequency than neurons in the adult (41), this theoretical result is amenable to experimental verification. Orientation tuning curves of the three neurons indicated by arrows in Fig. 3*A* are shown in Fig. 3 *B1–B3* again at 0.1 and 0.25 cycles per degree. Although the tuning of these neurons is less than that seen in adult cats with grating stimuli (42, 43), most studies of orientation tuning in striate cortex of visually inexperienced

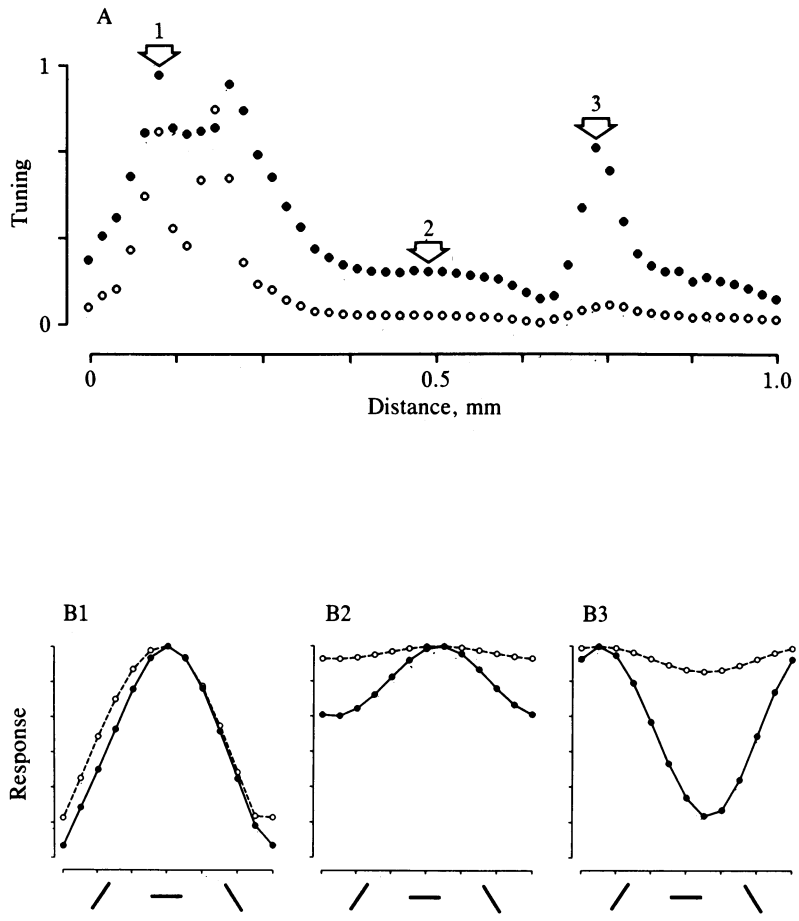

FIG. 3. (*A*) A measure of the sharpness of orientation tuning, as described in the text, for the vertical row of neurons labeled B at the top of Fig. 1. The sharpness of tuning is shown for two spatial frequencies, 0.1 cycles per degree (○) and 0.25 cycles per degree (●). (*B1–B3*) Normalized orientation tuning curves for the three neurons indicated by arrows 1–3 in *A*. The tuning curves were calculated at two spatial frequencies, 0.1 cycles per degree (○) and 0.25 cycles per degree (●).

kittens have reported broader tuning than in the adult (3, 4, 6, 44–48).

It is important to note that the retinotopic mapping of the RGC mosaic onto the cortex need not be precise for a columnar organization of preferred orientations to result. Simulations were performed in which the strict retinotopy was relaxed, and the afferent fibers entered the cortex at quasi-random positions within circular regions (of uniform probability density) centered on the retinotopic position of their receptive fields. When the diameters of this region were up to one-half the mean distance to the nearest-neighbor afferent, the pattern of orientation columns was quite similar to that shown in Fig. 1. When the retinotopy was further relaxed, the pattern of preferred orientation on the cortical surface changed substantially but remained columnar in organization.

DISCUSSION

Previous simulations of the development of orientation columns (49–53), as well as some models presented without simulation (54–56), have had in common a dependence on intracortical interactions. This stands in contrast to the simulation presented here, where the blueprint of the columns was determined by the RGC mosaic without the involvement of intracortical interactions. The orientation tuning of the simulated cortical neurons can arise from two types of asymmetries in their receptive fields: (*i*) elongation parallel to the preferred orientation and (*ii*) a spatial offset of the "center of mass" of the on- and off-center inputs perpendicular to the preferred orientation (7). Although the spread of visual afferents (distance function) and the RCG receptive fields are taken as radially symmetric, these asymmetries in cortical receptive fields result from the discreteness of the RGC mosaic. The tangential organization of the columns, as well as the tendency of nearby neurons to have similar preferred orientations, is due to the fact that closely spaced cortical neurons receive similar patterns of convergence of afferent inputs. One consequence of this mechanism is that during development each eye will establish its own set of orientation columns. For the preferred orientations from the two eyes to correspond, an instructive process involving visual experience would be required. This could occur with the preferred orientation assuming the value determined by the dominant eye or a weighted average of the input from both eyes. It would then be expected that in animals raised without a binocular visual experience the preferred orientations of neurons in striate cortex would not be the same for both eyes. This is, in fact, in agreement with experimental results. Blakemore and Van Sluyters (4, 57) and Movshon (58) studied the interocular differences of preferred orientation in striate cortex neurons of binocularly deprived and reverse-sutured kittens. In contrast to animals with a normal visual experience, they found large differences in the preferred orientations from the two eyes, which in some neurons were virtually orthogonal.

The mechanism I propose here for the origin of the orientation columns involves no assumptions about the experience-dependent process by which the sharp orientation tuning of adult neurons develops from the more broadly

tuned responses of young kittens (4, 6, 45–48, 57–67). However, I have shown in a previous report (7) that sharply tuned simple cell responses can be synthesized by the summation of appropriate patterns of afferent input, in agreement with the model of Hubel and Wiesel (2). This suggests that experience-dependent modification of the afferent synapses, rather than intracortical synapses, could be the primary mechanism for enhancement of orientation tuning. The mapping of the RGC mosaic onto the cortex can thus be viewed as performing two crucial functions: defining the blueprint for the orientation columns and providing a substrate of multiple afferent inputs to be sculpted by visual experience.

COMPARISON WITH MONKEY

In the monkey, striate cortex receives the bulk of its geniculate input from two cell types: the P cells from the parvocellular layers and the M cells from the magnocellular layers (68–70). The P cells are distinguished by smaller receptive fields and a higher retinal density than the M cells (71–77), which is somewhat analogous to the relationship between the X and Y cells of the cat. However, with regard to their spatial summation properties, the P cells are X-like, whereas the M cells can be either X-like or Y-like (74, 75, 78–81). Further comparison, based on measurements of contrast sensitivity, have led Kaplan, Shapley, and co-workers to suggest that, in fact, it is the linearly summing M cells that are homologous to the X cells of the cat (74, 78, 79, 82).

The geniculocortical projections of the P and M cells are segregated; the parvocellular layers project mainly to layers IVA and IV$C\beta$, and the magnocellular cells project mainly to layer IV$C\alpha$ (68–70). Physiological (83–85) and deoxyglucose (85, 86) studies show that most neurons in the striate cortex parvocellular-receiving layers are untuned to orientation, whereas those in the magnocellular-receiving layer are tuned and have an orderly arrangement of preferred orientations. This suggests that in monkeys the M-cell retinal mosaic is responsible for determining the pattern of the orientation columns. A third component of the monkey geniculostriate projection arises from the thin, sparsely populated intercalated layers of the LGN. This component has been shown to terminate in the supragranular regions characterized by high cytochrome oxidase activity and unoriented color-coding neurons, the cytochrome oxidase blobs (85–92).

The mechanisms proposed here for the origin of the orientation columns can, with a further assumption, also explain the absence of orientation tuning in the blobs. Given the scarcity of neurons in the intercalated layers of the LGN, which provide the afferent input to the blobs, it is conceivable that the blobs are induced by the cortical projection of the intercalated layer neurons in a one-for-one manner. Under this assumption, the blobs would be defined by the nonoverlapping arborizations of widely spaced afferents, and the blob neurons would receive afferent input from only a single geniculate fiber. There would, thus, be no convergence of elements of the RGC mosaic to define a preferred orientation or provide a substrate of afferents to be sculpted by visual experience. The blob neuron-receptive field properties would be defined by their single afferent input and would remain so throughout the period of susceptibility to environmental modification. A one-for-one induction of blobs by intercalated layer afferents is also consistent with the observation that all neurons recorded in a given blob have the same color opponency (92), which presumably would be defined by the opponency of the inducing afferent. This speculation leads to a view of the blobs as a reproduction on the cortex of the retinal mosaic of ganglion cells that project to the intercalated layers of the LGN; the discreteness of the mosaic is preserved by the relatively low density and narrow spread of their axon arbors in the supragranular layers.

I thank James Gordon, Ehud Kaplan, Bruce Knight, Floyd Ratliff, and Robert Shapley for support, encouragement, and critical reading of the manuscript. This work was supported by Grants RO1-EY4888, EY1472, and EY1428 from the National Eye Institute.

1. Hubel, D. H. & Wiesel, T. N. (1962) *J. Physiol. (London)* **160,** 106–154.
2. Hubel, D. H. & Wiesel, T. N. (1963) *J. Physiol. (London)* **165,** 559–568.
3. Hubel, D. H. & Wiesel, T. N. (1963) *J. Neurophysiol.* **26,** 994–1002.
4. Blakemore, C. & Van Sluyters, R. C. (1975) *J. Physiol. (London)* **248,** 663–716.
5. Sherk, H. & Stryker, M. P. (1976) *J. Neurophysiol.* **39,** 63–70.
6. Albus, K. & Wolf, W. (1984) *J. Physiol. (London)* **348,** 153–185.
7. Soodak, R. E. (1986) *Proc. Natl. Acad. Sci. USA* **83,** 9259–9263.
8. Wässle, H., Boycott, B. B. & Illing, R.-B. (1981) *Proc. R. Soc. London Ser. B* **212,** 177–195.
9. Wässle, H., Peichl, L. & Boycott, B. B. (1981) *Proc. R. Soc. London Ser. B* **212,** 157–175.
10. Boycott, B. B. & Wässle, H. (1974) *J. Physiol. (London)* **240,** 397–419.
11. Wässle, H., Levick, W. R. & Cleland, B. G. (1975) *J. Comp. Neurol.* **159,** 419–438.
12. Enroth-Cugell, C. & Robson, J. G. (1966) *J. Physiol. (London)* **187,** 517–552.
13. Cleland, B. G., Dubin, M. W. & Levick, W. R. (1971) *J. Physiol. (London)* **217,** 473–496.
14. Hochstein, S. & Shapley, R. M. (1976) *J. Physiol. (London)* **262,** 237–264.
15. Hochstein, S. & Shapley, R. M. (1976) *J. Physiol. (London)* **262,** 265–284.
16. Hubel, D. H. & Wiesel, T. N. (1961) *J. Physiol. (London)* **155,** 385–398.
17. Kaplan, E., Marcus, S. & So, Y. T. (1979) *J. Physiol. (London)* **294,** 561–580.
18. So, Y. T. & Shapley, R. M. (1981) *J. Neurophysiol.* **45,** 107–120.
19. Kaplan, E. & Shapley, R. M. (1984) *Exp. Brain Res.* **55,** 111–116.
20. Tusa, R. J., Palmer, L. A. & Rosenquist, A. C. (1978) *J. Comp. Neurol.* **177,** 213–236.
21. Ferster, D. & LeVay, S. (1978) *J. Comp. Neurol.* **182,** 923–944.
22. Humphrey, A. L., Sur, M., Uhlrich, D. J. & Sherman, S. M. (1985) *J. Comp. Neurol.* **233,** 159–189.
23. Stone, J. & Dreher, B. (1973) *J. Neurophysiol.* **36,** 551–567.
24. Bullier, J. & Henry, G. H. (1979) *J. Neurophysiol.* **42,** 1264–1270.
25. Tanaka, K. (1983) *J. Neurophysiol.* **49,** 1303–1318.
26. Freund, T. F., Martin, K. A. C. & Whitteridge, D. (1985) *J. Comp. Neurol.* **242,** 263–274.
27. Hammond, P. (1974) *J. Physiol. (London)* **242,** 99–118.
28. Levick, W. R. & Thibos, L. N. (1980) *Nature (London)* **286,** 389–390.
29. Levick, W. R. & Thibos, L. N. (1982) *J. Physiol. (London)* **329,** 243–261.
30. Soodak, R. E., Shapley, R. M. & Kaplan, E. (1986) *J. Neurophysiol.*, in press.
31. Leventhal, A. G. (1983) *J. Comp. Neurol.* **220,** 476–483.
32. Leventhal, A. G. (1985) in *Models of the Visual Cortex*, eds. Rose, D. & Dobson, V. G. (Wiley, New York), pp. 380–389.
33. Schall, J. D., Vitek, D. J. & Leventhal, A. G. (1986) *J. Neurosci.* **6,** 823–836.
34. Tottell, R. B. H., Silverman, M. S., Switkes, E. & De Valois, R. L. (1982) *Science* **218,** 902–904.
35. Van Essen, D. C., Newsome, W. T. & Maunsell, J. H. R. (1984) *Vision Res.* **24,** 429–448.
36. Hubel, D. H. & Wiesel, T. N. (1974) *J. Comp. Neurol.* **158,** 267–294.
37. Albus, K. (1975) *Exp. Brain Res.* **24,** 181–202.
38. Albus, K. (1985) in *Models of the Visual Cortex*, eds. Rose, D. & Dobson, V. G . (Wiley, New York), pp. 485–491.
39. Blasdel, G. G. & Salama, G. (1986) *Nature (London)* **321,** 579–585.
40. Leventhal, A. G. & Hirsch, H. V. B. (1980) *J. Neurophysiol.* **43,** 1111–1132.

41. Derrington, A. M. & Fuchs, A. F. (1981) *J. Physiol. (London)* **316,** 1–10.
42. Campbell, F. W., Cleland, B. G., Cooper, G. F. & Enroth-Cugell, C. (1968) *J. Physiol. (London)* **198,** 237–250.
43. DeValois, K. K., DeValois, R. L. & Yund, E. W. (1979) *J. Physiol. (London)* **291,** 483–505.
44. Barlow, H. B. & Pettigrew, J. D. (1971) *J. Physiol. (London)* **218,** 98P–101P (abstr.).
45. Pettigrew, J. D. (1974) *J. Physiol. (London)* **237,** 49–74.
46. Imbert, M. & Buisseret, P. (1975) *Exp. Brain Res.* **22,** 25–36.
47. Buisseret, P. & Imbert, M. (1976) *J. Physiol. (London)* **255,** 511–525.
48. Bonds, A. B. (1979) in *Developmental Neurobiology of Vision*, ed. Freeman, R. D. (Plenum, New York), pp. 31–41.
49. von der Malsburg, C. (1973) *Kybernetik* **14,** 85–100.
50. Swindale, N. V. (1982) *Proc. R. Soc. London Ser. B* **215,** 211–230.
51. von der Malsburg, C. & Cowan, J. D. (1982) *Biol. Cybern.* **45,** 49–56.
52. Cowan, J. D. & von der Malsburg, C. (1985) in *Models of the Visual Cortex*, eds. Rose, D. & Dobson V. G. (Wiley, New York), pp. 462–472.
53. Linsker, R. (1986) *Proc. Natl. Acad. Sci. USA* **83,** 8390–8394.
54. Braitenberg, V. & Braitenberg, C. (1979) *Biol. Cybern.* **33,** 179–186.
55. Dow, B. M. & Bauer, R. (1984) *Biol. Cybern.* **49,** 189–200.
56. Braitenberg, V. (1985) in *Models of the Visual Cortex*, eds. Rose, D. & Dobson, V. G. (Wiley, New York), pp. 479–484.
57. Blakemore, C. & Van Sluyters, R. C. (1974) *J. Physiol. (London)* **237,** 195–216.
58. Movshon, J. A. (1976) *J. Physiol. (London)* **261,** 125–174.
59. Blakemore, C. & Cooper, G. F. (1970) *Nature (London)* **228,** 477–478.
60. Hirsch, H. V. B. & Spinelli, D. N. (1970) *Science* **168,** 869–871.
61. Nass, M. M. & Cooper, L. N. (1975) *Biol. Cybern.* **19,** 1–18.
62. Pérez, R., Glass, L. & Shlaer, R. (1975) *J. Math. Biol.* **1,** 275–288.
63. Stryker, M. P., Sherk, H., Leventhal, A. G. & Hirsch, H. V. B. (1978) *J. Neurophysiol.* **41,** 896–909.
64. Cooper, L. N., Liberman, F. & Oja, E. (1979) *Biol. Cybern.* **33,** 9–28.
65. Frégnac, Y. (1979) in *Developmental Neurobiology of Vision*, ed. Freeman, R. D. (Plenum, New York), pp. 51–62.
66. Rauschecker, J. P. & Singer, W. (1981) *J. Physiol. (London)* **310,** 215–239.
67. Singer, W. (1985) *Vision Res.* **25,** 389–396.
68. Hubel, D. H. & Wiesel, T. N. (1972) *J. Comp. Neurol.* **146,** 421–450.
69. Hendrickson, A. E., Wilson, J. R. & Ogren, M. P. (1978) *J. Comp. Neurol.* **182,** 123–136.
70. Blasdel, G. G. & Lund, J. S. (1983) *J. Neurosci.* **3,** 1389–1413.
71. Wiesel, T. N. & Hubel, D. H. (1966) *J. Neurophysiol.* **29,** 1115–1156.
72. Gouras, P. (1969) *J. Physiol. (London)* **204,** 407–419.
73. De Monasterio, F. M. & Gouras, P. (1975) *J. Physiol. (London)* **251,** 167–195.
74. Kaplan, E. & Shapley, R. M. (1982) *J. Physiol. (London)* **330,** 125–143.
75. Derrington, A. M. & Lennie, P. (1984) *J. Physiol. (London)* **357,** 219–240.
76. Perry, V. H., Oehler, R. & Cowey, A. (1984) *Neuroscience* **12,** 1101–1123.
77. Perry, V. H. & Cowey, A. (1985) *Vision Res.* **25,** 1795–1810.
78. Shapley, R. M., Kaplan, E. & Soodak, R. E. (1981) *Nature (London)* **292,** 543–545.
79. Kaplan, E. & Shapley, R. M. (1986) *Proc. Natl. Acad. Sci. USA* **83,** 2755–2757.
80. Blakemore, C. & Vital-Durand, F. (1981) *J. Physiol. (London)* **320,** 17P–18P (abstr.).
81. Sherman, S. M., Schumer, R. & Movshon, J. A. (1984) *Soc. Neurosci. Abstr.* **10,** 296.
82. Shapley, R. M. & Perry, V. H. (1986) *Trends Neuro. Sci.* **9,** 229–235.
83. Bullier, J. & Henry, G. F. (1980) *J. Comp. Neurol.* **193,** 913–935.
84. Blasdel, G. G. & Fitzpatrick, D. (1984) *J. Neurosci.* **4,** 880–895.
85. Livingstone, M. S. & Hubel, D. H. (1984) *J. Neurosci.* **4,** 309–356.
86. Humphrey, A. L. & Hendrickson, A. E. (1983) *J. Neurosci.* **3,** 345–358.
87. Horton, J. C. & Hubel, D. H. (1981) *Nature (London)* **292,** 762–764.
88. Livingstone, M. S. & Hubel, D. H. (1982) *Proc. Natl. Acad. Sci. USA* **79,** 6098–6101.
89. Fitzpatrick, D., Itoh, K. & Diamond, I. T. (1983) *J. Neurosci.* **3,** 673–702.
90. Weber, J. T., Huerta, M. F., Kaas, J. H. & Harting, J. K. (1983) *J. Comp. Neurol.* **213,** 135–145.
91. Kennedy, H., Bullier, J. & Dehay, C. (1985) *Exp. Brain Res.* **61,** 204–209.
92. Ts'o, D. Y., Gilbert, C. G. & Wiesel, T. N. (1986) *Soc. Neurosci. Abstr.* **12,** 1497.